

Ground-state properties of finite nuclei with astrophysical interest in extreme magnetic fields, via covariant density functional theory

Ioannis Mavroudis, PhD candidate

School of Physics
Aristotle University of Thessaloniki

34th Annual Symposium of the Hellenic Nuclear Physics Society
June 5, 2026



Outline

- 1 Introduction and Motivation
- 2 Theoretical Framework
- 3 Results (Preliminary)
- 4 Summary
- 5 Collaborators and Acknowledgements
- 6 Selected References

Outline

- 1 Introduction and Motivation
- 2 Theoretical Framework
- 3 Results (Preliminary)
- 4 Summary
- 5 Collaborators and Acknowledgements
- 6 Selected References

Astrophysical Laboratories: Magnetars & Explosive Transients

- **Extreme Magnetic Fields:** Magnetars host surface fields of $B \sim 10^{15}$ G. However, transient internal fields up to $B \sim 10^{17} - 10^{18}$ G can be generated dynamically in **Core-Collapse Supernovae (CCSNe)** and **Neutron Star Mergers (NSMs)**.
- **Explosive Nucleosynthesis:** These highly magnetized, extreme-density environments are the primary cosmic sites for rapid neutron (r -process) and rapid proton (rp -process) capture.

The Core Question

How do these extreme transient fields fundamentally change the structure of finite nuclei being synthesized in these stellar explosive environments?

Explosive Environments & Selected Nuclei

- So, understanding ground-state bulk properties, e.g., deformation, binding energy and radii, are critical for accurately modeling nucleosynthesis yields and reaction rates in explosive sites.

Selected Nuclei in this Study:

- ${}^{64}_{32}\text{Ge}_{32}$ (Type I X-ray Bursts): A key waiting-point nucleus in the rp-process on accreting neutron stars. $N = Z$ nucleus on rp-path, where further proton capture stalls, waiting β^+ decays to proceed.
- ${}^{130}_{48}\text{Cd}_{82}$ (CCSNe & NSMs): A classic neutron-rich waiting-point nucleus near the $N = 82$ shell closure. Neutron magic shell isotones $N = 50, 82, 126$, crucial for explaining peaks in the observed abundance distribution. Neutron capture is suppressed, waiting β^- decays to occur.

Outline

- 1 Introduction and Motivation
- 2 Theoretical Framework**
- 3 Results (Preliminary)
- 4 Summary
- 5 Collaborators and Acknowledgements
- 6 Selected References

Incorporating the External Magnetic Field

- To study finite nuclei in superstrong magnetic fields ($B \sim 10^{17}$ G), we define a uniform field along the z -axis: $\mathbf{B} = B\hat{z}$.

There are two primary theoretical frameworks to model this environment:

1. Non-Relativistic (Skyrme DFT)

- Based on the derived Hamiltonian \hat{h}_q .
- Magnetic coupling must be added explicitly.

2. Relativistic (CDFT)

- Based on the Dirac equation and meson exchange (σ, ω, ρ).
- Magnetic coupling arises *naturally*.

The Effective Lagrangian - Relativistic Framework I

- CDFT begins with an effective Lagrangian encompassing nucleons, meson fields (σ, ω, ρ), and the electromagnetic field:

$$\mathcal{L} = \mathcal{L}_N + \mathcal{L}_m + \mathcal{L}_{int} + \mathcal{L}_{BO} + \mathcal{L}_{BM} \quad (1)$$

where \mathcal{L}_N , the Lagrangian of the free nucleons, \mathcal{L}_m , the Lagrangian of the free mesons and EM field by p^+ , \mathcal{L}_{int} , the Lagrangian to describe interactions.

- \mathcal{L}_{int} differs on the selected parameter set. In this work, the **NL3*** and the **DD-ME2** are employed.
- Two new terms are introduced to couple the system with the external magnetic field:
(D. Peña Arteaga *et al.*, *Phys. Rev. C* **84**, 045806 (2011))

The Effective Lagrangian - Relativistic Framework II

1. Proton Orbital Coupling (Landau Dynamics):

$$\mathcal{L}_{BO} = -e\bar{\psi}\gamma^\mu A_\mu^{(e)}\psi \quad (2)$$

the coupling of p^+ orbital motion with the external magnetic field.

2. Intrinsic Dipole Magnetic Moment Coupling (Pauli Magnetism):

$$\mathcal{L}_{BM} = -\bar{\psi}\chi_{\tau_3}^{(e)}\psi \quad \text{where} \quad \chi_{\tau_3}^{(e)} = \kappa_{\tau_3}\mu_N\frac{1}{2}\sigma_{\mu\nu}F^{(e)\mu\nu} \quad (3)$$

the coupling of both p^+ and n^0 intrinsic dipole moments with the external magnetic field.

where $\sigma_{\mu\nu} = \frac{i}{2}[\gamma_\mu, \gamma_\nu]$, $\mu_N = \frac{e\hbar}{2m}$, $\kappa_n = \frac{g_n}{2}$, $\kappa_p = \frac{g_p}{2} - 1$, $g_n = -3.8263$, and $g_p = 5.5856$.

The Dirac Equation & Symmetry Breaking I

- Pairing correlations are neglected, so no additional term into the energy functional
- Minimizing the energy functional with respect to the density yields the stationary Dirac equation for the nucleons and Klein-Gordon equations for mesons:

$$\left[\boldsymbol{\alpha} \cdot (-i\nabla - \mathbf{V}) + V_0 + \beta(m + S) + \beta\chi_{\tau_3}^{(e)} \right] \psi_i = \epsilon_i \psi_i \quad (4)$$

S the scalar potential, V_μ the vector potential.

Physical Consequences of the Magnetic Field:

- **Loss of Spherical Symmetry:** The magnetic field breaks spherical symmetry for both the Dirac and Klein-Gordon equations, preserving only axial symmetry.

The Dirac Equation & Symmetry Breaking II

- **Time-Reversal Breaking:** The external field magnetic field breaks the time-reversal symmetry (T) in the intrinsic frame.
- **Kramers' Degeneracy Lifted:** Because T -symmetry is broken, the twofold degeneracy of states is removed. Solutions with positive and negative angular momentum projections ($\pm\Omega_j$) must be treated as completely separate states.

Nuclear Magnetism & Self-Consistency

The breaking of time-reversal symmetry profoundly alters the meson fields via the generation of spatial currents:

- **Induced Spatial Currents:** The ballistic dynamics of the nucleons generate non-vanishing spatial currents ($\mathbf{j}^p, \mathbf{j}^n$).
- **Time-Odd Meson Fields:** These currents act as direct sources for the spacelike (time-odd) components of the vector mesons ($\boldsymbol{\omega}$ and $\boldsymbol{\rho}$), inducing a phenomenon known as **nuclear magnetism**.

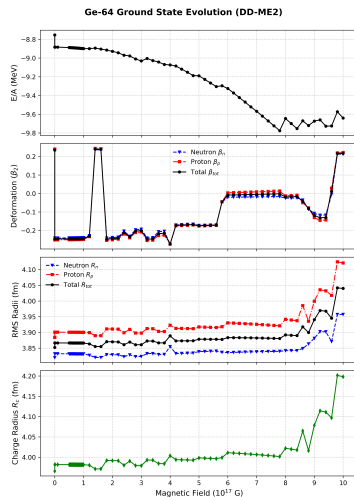
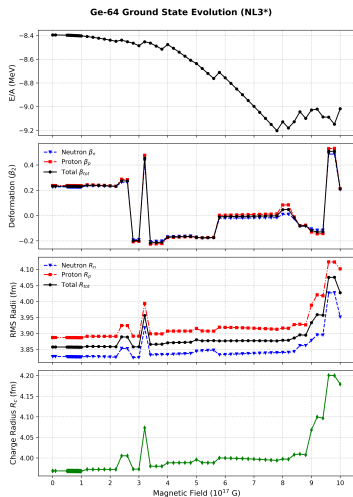
$$(-\Delta + m_\omega^2)\boldsymbol{\omega} = g_\omega(\mathbf{j}^p + \mathbf{j}^n) \quad (5)$$

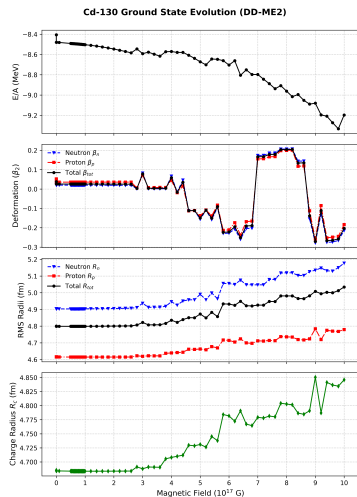
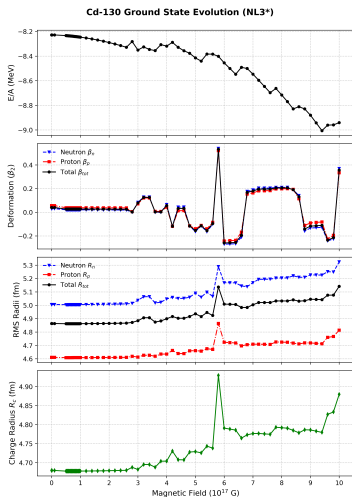
$$(-\Delta + m_\rho^2)\boldsymbol{\rho} = g_\rho(\mathbf{j}^p - \mathbf{j}^n) \quad (6)$$

The time-odd mean fields are governed by the exact same coupling constants (g_ω, g_ρ) as the time-even fields. The closed set of Dirac and Klein-Gordon equations is solved iteratively until the fully self-consistent solution converges.

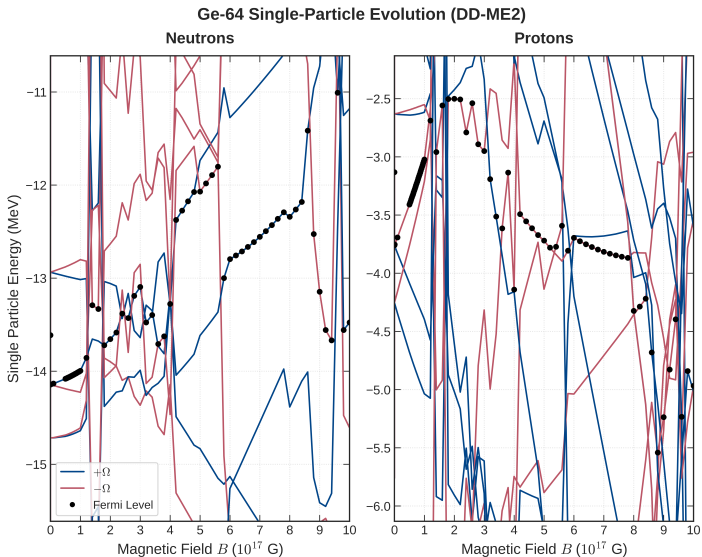
Outline

- 1 Introduction and Motivation
- 2 Theoretical Framework
- 3 Results (Preliminary)**
- 4 Summary
- 5 Collaborators and Acknowledgements
- 6 Selected References

Bulk Properties (BE/A , β_2 , Radii): ^{64}Ge 

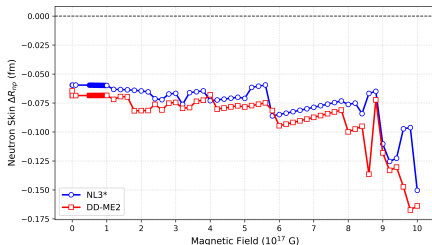
Bulk Properties (BE/A , β_2 , Radii): ^{130}Cd 

Microscopic Origins: Single-Particle Levels

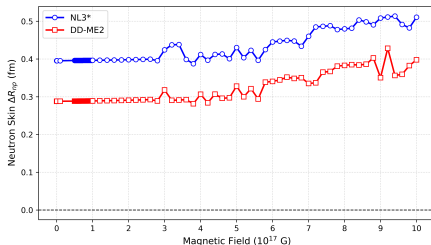


Evolution of the Neutron Skin Thickness

Ge-64 Neutron Skin Evolution (NL3* vs DD-ME2)



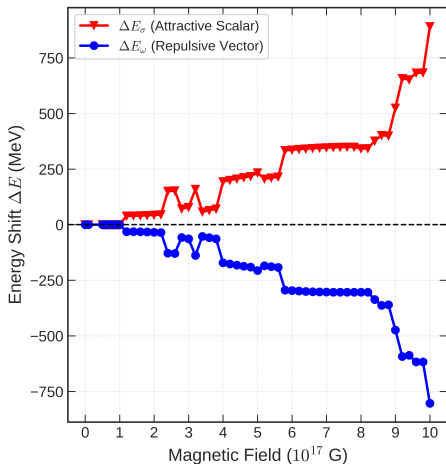
Cd-130 Neutron Skin Evolution (NL3* vs DD-ME2)



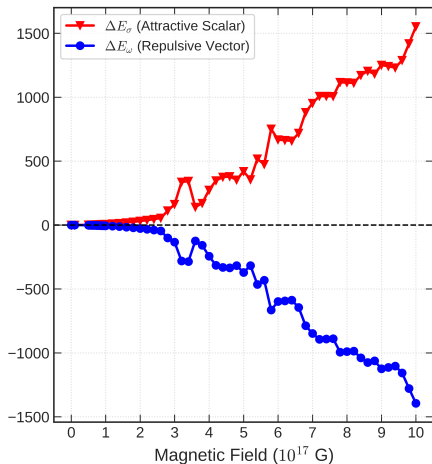
Meson Field Response (NL3*)

Dominant Meson Field Responses (σ vs. ω) (NL3*)

^{64}Ge ($N = Z = 32$)



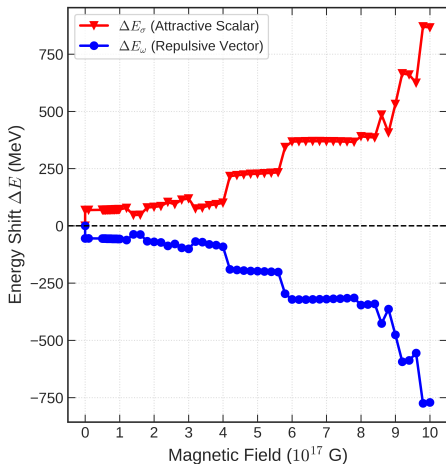
^{130}Cd ($N = 82, Z = 48$)



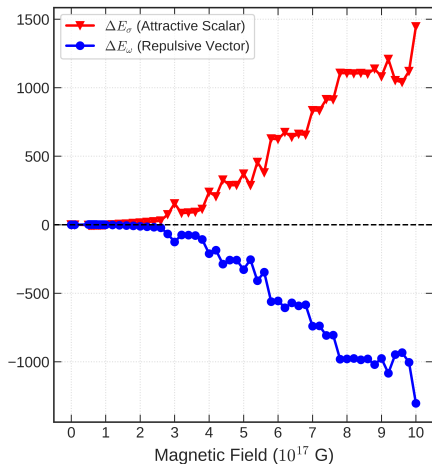
Meson Field Response (DD-ME2)

Dominant Meson Field Responses (σ vs. ω) (DD-ME2)

^{64}Ge ($N = Z = 32$)



^{130}Cd ($N = 82, Z = 48$)

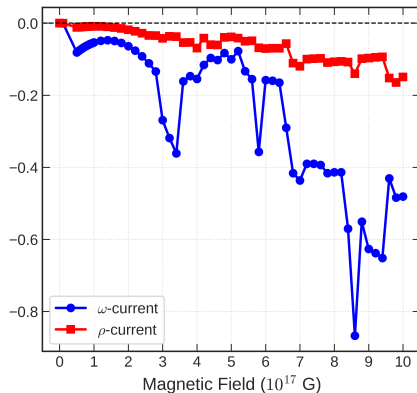
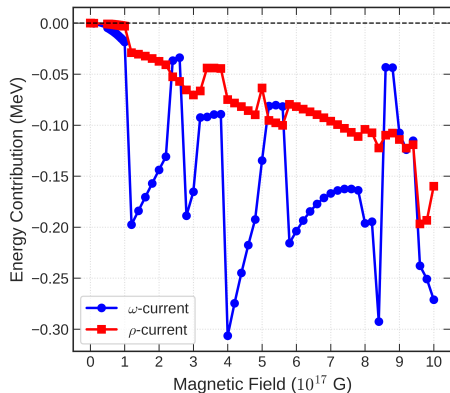


Time-Reversal Breaking: Induced Meson Currents (NL3*)

Time-Reversal Breaking Meson Currents (NL3*)

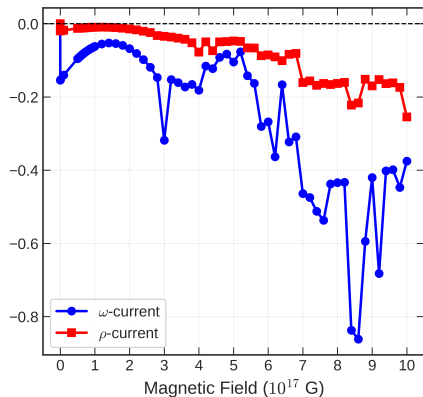
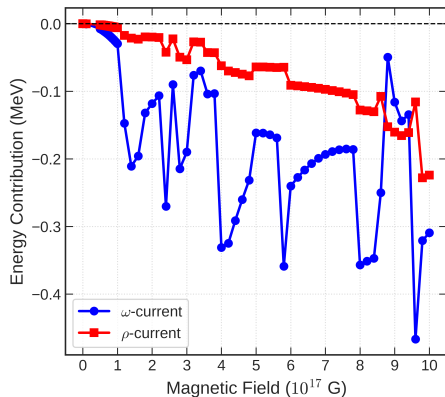
^{64}Ge ($N=Z=32$)

^{130}Cd ($N=82, Z=48$)



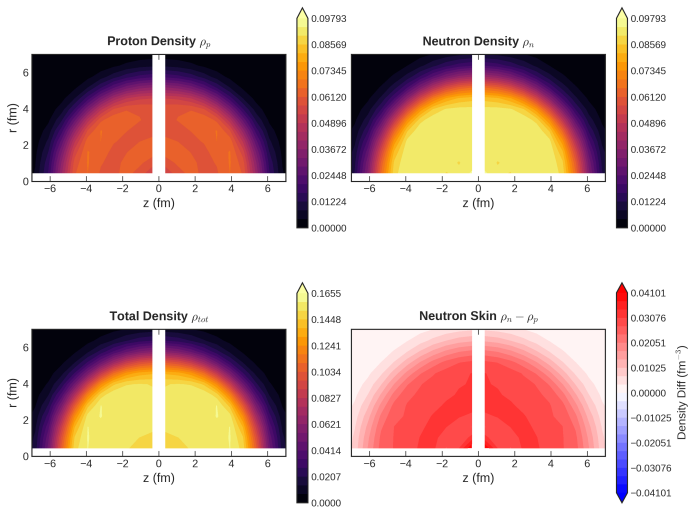
Time-Reversal Breaking: Induced Meson Currents (DD-ME2)

Time-Reversal Breaking Meson Currents (DD-ME2)
 ^{64}Ge ($N = Z = 32$) ^{130}Cd ($N = 82, Z = 48$)



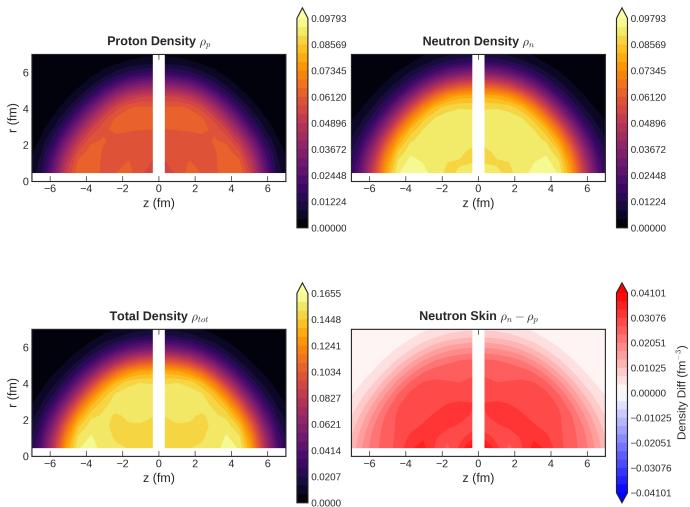
Evolution of Nuclear Density: ^{130}Cd ($B = 0$ G)

Cd-130 Spatial Densities at $B = 0.0000 \times 10^{17}$ G (DD-ME2)



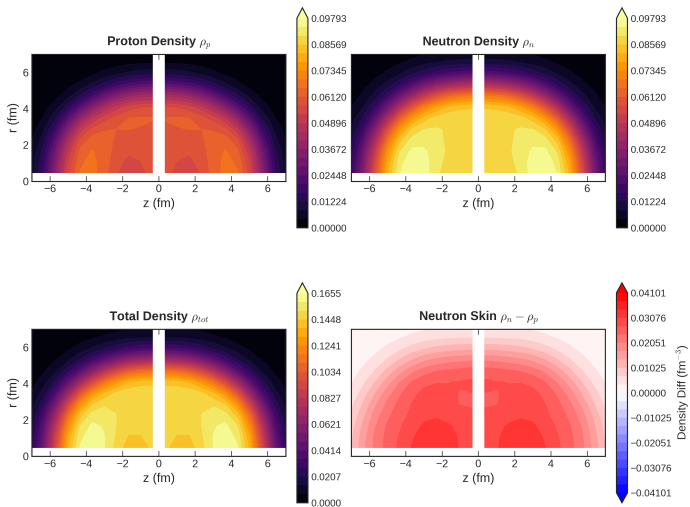
Evolution of Nuclear Density: ^{130}Cd ($B = 4.4 \times 10^{17}$ G)

Cd-130 Spatial Densities at $B = 4.4000 \times 10^{17}$ G (DD-ME2)



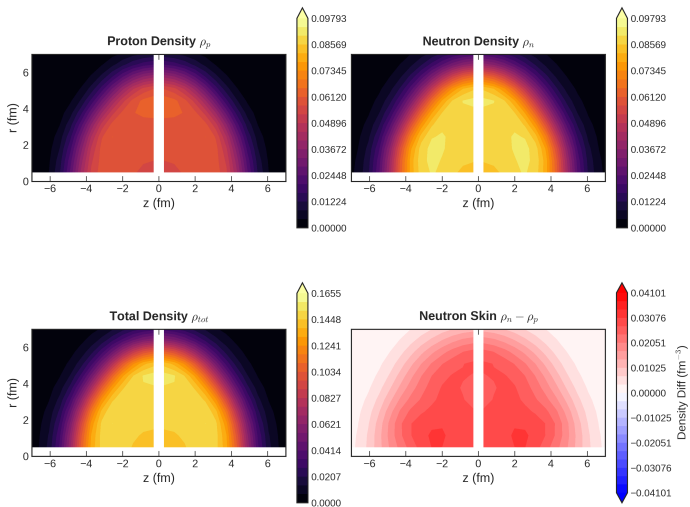
Evolution of Nuclear Density: ^{130}Cd ($B = 7.6 \times 10^{17}$ G)

Cd-130 Spatial Densities at $B = 7.6000 \times 10^{17}$ G (DD-ME2)



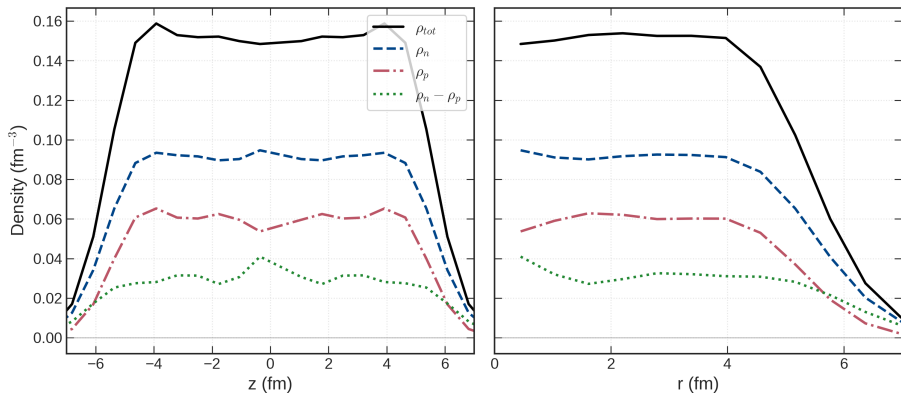
Evolution of Nuclear Density: ^{130}Cd ($B = 9.8 \times 10^{17}$ G)

Cd-130 Spatial Densities at $B = 9.8000 \times 10^{17}$ G (DD-ME2)



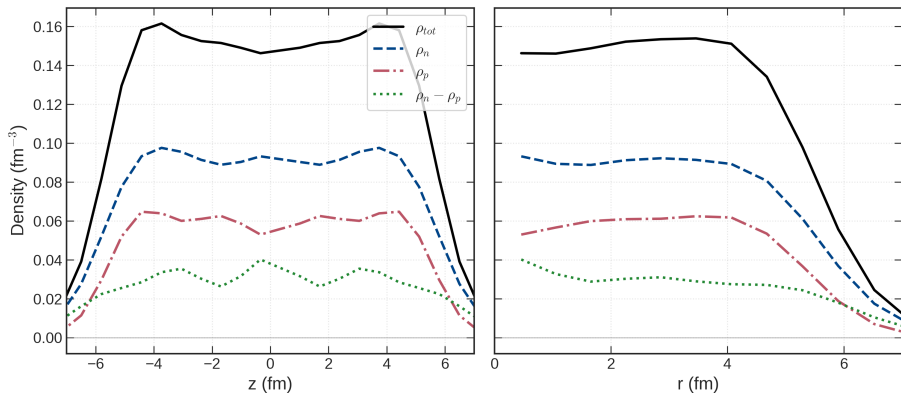
Density Profile ($B = 0$ G)

Cd-130 1D Densities at $B = 0.0 \times 10^{17}$ G (DD-ME2)
Pole ($\theta = 0^\circ$) **Equator ($\theta = 90^\circ$)**



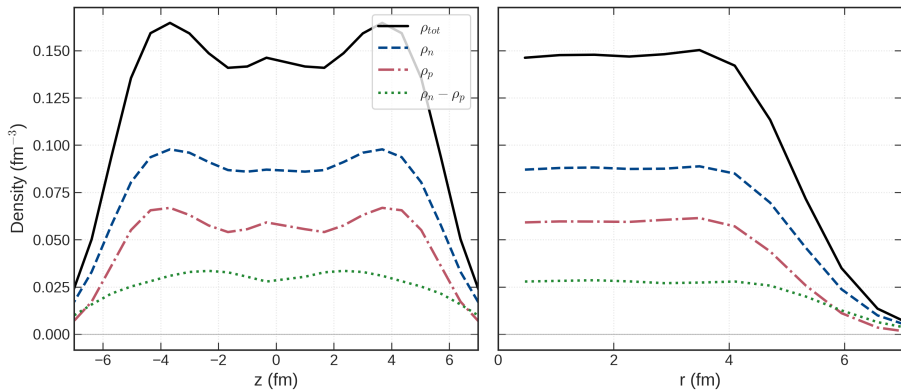
Density Profile ($B = 4.4 \times 10^{17}$ G)

Cd-130 1D Densities at $B = 4.4 \times 10^{17}$ G (DD-ME2)
 Pole ($\theta = 0^\circ$) Equator ($\theta = 90^\circ$)



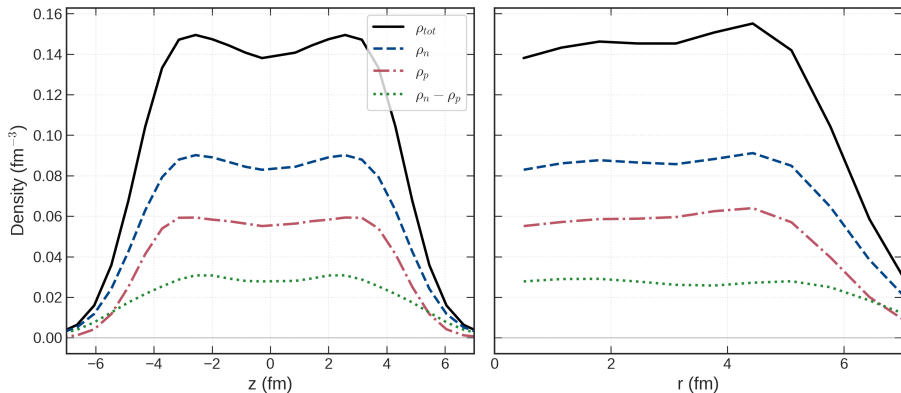
Density Profile ($B = 7.6 \times 10^{17}$ G)

Cd-130 1D Densities at $B = 7.6 \times 10^{17}$ G (DD-ME2)
 Pole ($\theta = 0^\circ$) Equator ($\theta = 90^\circ$)



Density Profile ($B = 9.8 \times 10^{17}$ G)

Cd-130 1D Densities at $B = 9.8 \times 10^{17}$ G (DD-ME2)
 Pole ($\theta = 0^\circ$) Equator ($\theta = 90^\circ$)



Outline

- 1 Introduction and Motivation
- 2 Theoretical Framework
- 3 Results (Preliminary)
- 4 Summary**
- 5 Collaborators and Acknowledgements
- 6 Selected References

Summary

Microscopic Origins: Symmetry Breaking

- Superstrong magnetic fields ($B \sim 10^{17}$ - 10^{18} G) fundamentally break time-reversal symmetry, lifting Kramers' degeneracy.
- The preservation of axial symmetry permits critical single-particle level crossings at the Fermi surface.

Macroscopic Consequences: Structural Evolution

- Sudden quantum reoccupations drive abrupt macroscopic **shape-phase transitions** (violent spikes in β_2 deformation).
- Landau quantization forces the transverse expansion of the proton fluid, altering RMS radii and inducing proton skins in symmetric nuclei like ^{64}Ge .

Outline

- 1 Introduction and Motivation
- 2 Theoretical Framework
- 3 Results (Preliminary)
- 4 Summary
- 5 Collaborators and Acknowledgements**
- 6 Selected References

Acknowledgements I

Scientific Collaboration

I would like to thank my professors and collaborators:

- **Charalampos Moustakidis**
- **Dimitrios Petrellis**
- **Georgios Lalazissis**
- **Petr Veselý**

for their discussions and guidance throughout this work.

Acknowledgements II

Computational Support

Results presented in this work have been produced using 1) GCP resources and 2) Aristotle HPC:

- 1 GCP resources were provided by the National Infrastructures for Research and Technology GRNET and funded by the EU Recovery and Resiliency Facility". (Project: Towards the Quantum Cosmos: Deep Learning and Quantum Computation for Neutron Star Physics - ToQC).
- 2 the Aristotle University of Thessaloniki (AUPH) High Performance Computing Infrastructure and Resources.

Outline

- 1 Introduction and Motivation
- 2 Theoretical Framework
- 3 Results (Preliminary)
- 4 Summary
- 5 Collaborators and Acknowledgements
- 6 Selected References**

Selected References I

 D. Peña Arteaga, M. Grasso, E. Khan, and P. Ring.

Nuclear structure in strong magnetic fields: Nuclei in the crust of a magnetar.
Phys. Rev. C **84**, 045806 (2011).

 J. U. Nabi, T. Bayram, G. Daraz, A. Kabir, and Ş. Şentürk.

The nuclear ground-state properties and stellar electron emission rates of ^{76}Fe , ^{78}Ni , ^{80}Zn , ^{126}Ru , ^{128}Pd and ^{130}Cd using RMF and pn-QRPA models.
Nucl. Phys. A **1015**, 122278 (2021).

 Q. Y. Hu, L. J. Wang, and Y. Sun.

Stellar weak rates of the rp-process waiting points: Effects of strong magnetic fields.
Phys. Rev. Lett. **135**, 042702 (2025).

 J. A. Maruhn, P.-G. Reinhard, P. D. Stevenson, and A. S. Umar.

The TDHF code Sky3D.
Comput. Phys. Commun. **185**, 2195–2216 (2014).

Selected References II



M. Stein, J. A. Maruhn, A. Sedrakian, and P.-G. Reinhard.
Carbon-oxygen-neon mass nuclei in superstrong magnetic fields.
Phys. Rev. C **94**, 035802 (2016).



D. Basilico, D. P. Arteaga, X. Roca-Maza, and G. Colò.
Outer crust of a cold non-accreting magnetar.
Phys. Rev. C **92**, 035802 (2015).



S. E. Agbemava, A. V. Afanasjev, D. Ray, and P. Ring.
Global performance of covariant energy density functionals: Ground state observables of even-even nuclei and the estimate of theoretical uncertainties.
Phys. Rev. C **89**, 054320 (2014).